Technical Report No. 7-4

STRUCTURAL ANALYSIS OF PRESSURE HULLS: RIB-STIFFENED CYLINDRICAL SHELL WITH REINFORCED CIRCULAR PENETRATION

December 1969

Contract No. Nonr-4835(00)(X)

This research was sponsored by the Structural Mechanics Laboratory of the Naval Ship Research and Development Center under Naval Ship Systems Command Subproject SF 013 0303, Task 1936.

GENERAL TECHNOLOGY CORPORATION

ACCESSION for
CFSTI — WHITE SECTION ☑
DDC — BUFF SECTION ☐
UNANNOUNCED ☐
JUSTIFICATION ....

BY ....
DISTRIBUTION/AVAILABILITY CODES
DIST. | AVAIL. and/or SPECIAL

GENERAL TECHNOLOGY CORPORATION

RESEARCH AND DEVELOPMENT

48 Phillips Avenue
Lawrenceville, New Jersey 08648
Telephone: 609/896-1154

BUSINESS OFFICE

474 Summit Street
Elgin, Illinois 60120
Telephone: 312/695-1600

STRESS ANALYSIS • NOISE & VIBRATION • COMPOSITE MATERIALS

PLATES & SHELLS • ELASTICITY • STRUCTURAL DYNAMICS

THERMOELASTICITY • VISCOELASTICITY • PLASTICITY

WAVE PROPAGATION • FLUID DYNAMICS • AERODYNAMICS & FLUTTER

HEAT TRANSFER • DYNAMICS • BIOMECHANICS

GENERAL TECHNOLOGY CORPORATION

Technical Report No. 7-4

STRUCTURAL ANALYSIS OF PRESSURE HULLS:

RIB-STIFFENED CYLINDRICAL SHELL WITH REINFORCED CIRCULAR PENETRATION

by

R. F. Maye and L. M. Habip

Approved.

A. C. Eringen

A. C. Eringen
Senior Scientist, Consultant

December 1969

Contract No. Nonr-4835(00)(X)

This research was sponsored by the Structural Mechanics Laboratory of the Naval Ship Research and Development Center under Naval Ship Systems Command Subproject SF 013 0303, Task 1956.

LIST OF CONTENTS

LIST OF FIGURES

ABSTRACT

The main results of a structural analysis program concerning a conventional submarine pressure hull configuration consisting of a rib-stiffened cylindrical shell with a reinforced circular penetration under hydrostatic pressure are discussed. The mathematical solution in series form has been obtained by superposing the analytical solutions for (a) a long, unstiffened, and unperforated circular cylindrical thin shell, closed at the ends, under external hydrostatic pressure, (b) a long, unstiffened, and unperforated circular cylindrical thin shell under a prescribed number of arbitrary radial line loads, and (c) a long, unstiffened, circular cylindrical shallow thin shell under arbitrary loading along the boundary of a circular penetration. During the computation, following truncation of the series, the method of least squares is employed in solving for the integration constants determined by the boundary conditions prescribed along the ribs and the reinforced penetration. The analysis has been coded and the numerical results generated by the use of a digital computer for an unstiffened as well as a rib-stiffened shell with a reinforced penetration are presented and compared graphically with experimental data available from certain photoelastic model tests. The corresponding zone of influence of the penetration and the state of stress concentration about it are delineated.

NOMENCLATURE

a	=	subscript denoting solution for a plain, closed cylindrical shell under pressure.
a_i	=	coefficients depending on ν, κ, m; i = 1, 2, ... , 5
$a_m^{(s)}$	=	roots of Δ in lower half of complex plane; s = 1, 2, 3, 4
$\bar{a}_m^{(s)}$	=	complex conjugates of $a_m^{(s)}$
A	=	area of rib cross section
$\bar{A}$	=	area of ring cross section
A_m	=	integration constants
A'_m	=	integration constants
b	=	subscript denoting solution for a plain cylindrical shell under multiple radial line loads
b_i	=	coefficients depending on ν, κ, m; i = 1, 2, ... , 9
B	=	constant defined in Eq.(26)
B_{mji}	=	quantities defined in Eq.(35)
B_{mji}^{-1}	=	inverse of B_{mji}
c	=	subscript denoting solution for a plain cylindrical shell loaded along a circular penetration
c_{li}	=	rigid body displacement of i-th pair of ribs
C	=	torsional rigidity of ring
C_{mn}	=	functions defined in Eq.(31)
C'_{mn}	=	functions defined in Eq.(31)

C_{mni}	=	values of C_{mn} at $\eta = \ell_1/R$
C'_{mni}	=	values of C'_{mn} at $\eta = \ell_1/R$
D	=	extensional rigidity of shell defined in Eq.(13)
D_{mn}	=	functions defined in Eq.(31)
e	=	distance from 1-1 axis to intersection of ring and shell, Fig.3
e'	=	depth of rib of rectangular cross section, Fig.1
$\bar{e}$	=	distance from 1-1 axis to intersection of ring and membrane covering the opening, Fig.3
E	=	Young's modulus of shell material
E'	=	Young's modulus of rib material
$\bar{E}$	=	Young's modulus of ring material
$f(\eta)$	=	arbitrary function of η
$\bar{f}(\alpha)$	=	Fourier transform of $f(\eta)$
$f_i(\alpha)$	=	functions defined in Eq.(17); $i = 1, 2, 3$
F_i	=	radial, tangential, and transverse ring forces at $\rho = \bar{\rho}$; $i = 1, 2, 3$
$h(\phi)$	=	distance from plane of ring to shell middle surface at $\rho = \rho_0$, Fig.3
$\bar{h}$	=	value of $h(\phi)$ at $\phi = 0$
h_1	=	depth of ring, Fig.3
$H_k^{(1)}$	=	Hankel function of first kind and integer order k
i	=	subscript integer
i	=	$(-1)^{1/2}$

I = area moment of inertia of rib cross section relative to centroidal principal axis normal to plane of rib

I_1 = area moment of inertia of ring cross section relative to 1-1 axis, Fig.3

I_2 = area moment of inertia of ring cross section relative to 2-2 axis, Fig.3

$\underline{Im}$ = imaginary part

j = subscript integer

J_k = Bessel function of first kind and integer order k

k = subscript integer

K = flexural rigidity of shell defined in Eq.(13)

ℓ = subscript integer

ℓ_j = half distance between j-th pair of ribs; j = 1, 2, ... , N; j = 1, Fig.1

m = subscript integer

M = torsional ring moment at $\rho = \bar{\rho}$

M_η, M_θ,

$M_{\eta\theta}$, $M_{\theta\eta}$ = shell couple resultants in η, θ coordinate system, Fig.2

M_ρ, M_ϕ,

$M_{\rho\phi}$, $M_{\phi\rho}$ = shell couple resultants in ρ, ϕ coordinate system, Fig.2

n = subscript integer

N = number of pairs of ribs located symmetrically across transverse axis of shell

$\tilde{N}$ = dimensionless principal stress concentration factor defined in Eq.(4)

N_η, N_θ,

$N_{\eta\theta}$, $N_{\theta\eta}$ = shell stress resultants in η, θ coordinate system, Fig.2

N_ρ, N_ϕ,

$N_{\rho\phi}$, $N_{\phi\rho}$ = shell stress resultants in ρ, ϕ coordinate system, Fig.2

$\bar{N}_\rho$, $\bar{N}_\phi$, $\bar{N}_{\rho\phi}$ = stresses defined in Eq.(7)

$\tilde{N}_{\rho\phi}$ = effective membrane shear stress resultant, Fig.3

p = hydrostatic pressure, Fig.1

p' = radial load, Fig.2

P_m = interaction load amplitudes for single radial line load

P_{mj} = interaction load amplitudes for j-th pair of radial line loads

Q_η, Q_θ = shell transverse shear stress resultants in η, θ coordinate system, Fig.2

Q_ρ, Q_ϕ = shell transverse shear stress resultants in ρ, ϕ coordinate system, Fig.2

$\tilde{Q}_\rho$ = effective transverse shear stress resultant, Fig.3

$Q^{(s)}_{U_m}$, $Q^{(s)}_{V_m}$, $Q^{(s)}_{W_m}$ = residues

R = radius of shell middle surface, Fig.1

R' = centroidal radius of rib, Fig.1

$\underline{Re}$ = real part

s = superscript integer

$sgn(\eta)$ = 1 if $\eta > 0$; 0 if $\eta = 0$; -1 if $\eta < 0$

t = shell wall thickness, Fig.1

t' = width of rib of rectangular cross section, Fig.1

u = ring displacement in outward radial direction at $\rho = \bar{\rho}$

U = shell displacement in η direction, Fig.2

U_ρ, U_ϕ = shell displacements in ρ,ϕ coordinate system, Fig. 2

U_m = amplitudes of U_b

$\bar{U}_m$ = Fourier transform of U_m

v = ring displacement in tangential direction at $\rho = \bar{\rho}$

V = shell displacement in θ direction, Fig.2

V_m = amplitudes of V_b

$\bar{V}_m$ = Fourier transform of V_m

w = ring displacement in upward transverse direction at $\rho = \bar{\rho}$

w' = outward radial displacement of rib

W = shell displacement in radial direction, Fig.2

W_m = amplitudes of W_b

$\bar{W}_m$ = Fourier transform of W_m

z = shell thickness coordinate measured positive outward from middle surface

α	=	Fourier transform variable corresponding to η
β	=	material-curvature parameter defined in Eq.(27)
$\delta(\eta)$	=	Dirac delta function
δ_{ij}	=	Kronecker delta; 0 if $i \neq j$; 1 if $i = j$
$\Delta(\alpha)$	=	function defined in Eq.(17)
η, θ	=	dimensionless cylindrical coordinates, Fig.1
$(\ )_{,\eta}$	=	partial derivative with respect to η
$(\ )_{,\theta}$	=	partial derivative with respect to θ
η_j'	=	functions defined in Eq.(24)
η_j''	=	functions defined in Eq.(24)
κ	=	constant defined in Eq.(12)
$\lambda_{nm\ell}$	=	functions defined in Eq.(28)
ν	=	Poisson's ratio of shell material
ν'	=	Poisson's ratio of rib material
$\bar{\nu}$	=	Poisson's ratio of ring material
ξ	=	function defined in Eq.(21)
ξ_j'	=	functions defined in Eq.(24)
ξ_j''	=	functions defined in Eq.(24)
ξ_{ji}'	=	values of ξ_j' at $\eta = \ell_i/R$
ξ_{ji}''	=	values of ξ_j'' at $\eta = \ell_i/R$
ρ, ϕ	=	surface-polar coordinates, Fig.1
$(\ )_{,\rho}$	=	partial derivative with respect to ρ

$( ),_{\phi}$	=	partial derivative with respect to ϕ
ρ_o	=	outer radius of reinforced penetration, Fig.1
$\bar{\rho}$	=	distance from transverse axis of shell to 1-1 axis, Fig.3
$\sigma_{\rho}, \sigma_{\phi}, \tau_{\rho\phi}$	=	stresses in ρ, ϕ coordinate system
σ_1, σ_2	=	principal stresses for rib-stiffened shell with reinforced penetration
$\bar{\sigma}_1, \bar{\sigma}_2$	=	principal stresses for plain shell
ϕ	=	complex potential function
∇^2	=	Laplacian operator

1. INTRODUCTION

Current interest in the structural analysis of deep diving manned submersibles and of submerged habitats, such as naval or commercial submarines and installations and oceanographic research vehicles and laboratories, is due to evolving tactical concepts and emerging economic and scientific goals in the development of underwater resources and the exploration of the underwater environment. It is generally recognized that the presence of structural penetrations, such as missile tubes, hatches, locks, observation ports, valves, and various other functional connections, constitutes a source of weakness in any pressure hull. Related problems arise in the pressure vessel and pipeline technologies where structural intersections are common. A comprehensive review[1] of past research on the subject is available.

In recent years, considerable analytical and experimental data on the stress analysis of pressure vessels with intersections have been obtained[2-4] in support of programs for the development of associated design codes. The results make possible the planning of further experiments and the partial verification of information obtained by more powerful methods[5] of computational stress analysis.

Pressure hulls with penetrations have also been investigated by both analytical and experimental means in the course of recent programs of submarine structural research involving conventional hull configurations. The present work, part of such efforts, concerns the analysis of a rib-stiffened cylindrical shell with a reinforced circular penetration subjected to hydrostatic pressure. The special cases of a rib-stiffened shell with an unreinforced penetration[6], including the presence of multiple stiffeners[7], and that of an unstiffened shell with a reinforced penetration[8] have been reported earlier. Other numerical results[9] on the last problem are also available. Experimentally, all of the above pressure hull configurations have been studied.[10-12]

The configuration considered here, as shown in Fig.1, consists of a long, circular cylindrical, thin shell of uniform wall thickness t and middle surface radius R, closed at the ends, with several identical, internal, circumferential stiffeners of centroidal radius R', and a single, centrally located, reinforced circular penetration of outer radius ρ_0, closed by a flat membrane. The loading consists of external hydrostatic pressure p, and the deformation is taken small and static. The dimensionless axial and circumferential coordinates, η and θ, respectively, are centered at the point of intersection 0 of the longitudinal and transverse axes of the shell, as shown in Fig.1, with $R\eta$ a measure of length. The corresponding axial, circumferential, and radial displacements, U, V, and W, respectively, stress resultants N_η, N_θ, $N_{\eta\theta}$, $N_{\theta\eta}$, Q_η, Q_θ, couple resultants M_η, M_θ, $M_{\eta\theta}$, $M_{\theta\eta}$, and an arbitrary radial load p' for an element of the shell middle surface are indicated in Fig.2 where the intended sense of a couple is also given. The surface coordinates ρ and ϕ, representing polar coordinates defined in the plane obtained by developing[2] the cylindrical middle surface, are centered at the point 0' directly above point 0, at the intersection of the main generator and the transverse axis of the shell, as shown in Fig.1, with

$$R\eta = \rho\cos\phi, \qquad R\theta = \rho\sin\phi. \tag{1}$$

The corresponding displacements U_ρ, U_ϕ, stress resultants N_ρ, N_ϕ, $N_{\rho\phi}$, $N_{\phi\rho}$, Q_ρ, Q_ϕ, and couple resultants M_ρ, M_ϕ, $M_{\rho\phi}$, $M_{\phi\rho}$ for an element of the shell middle surface are indicated in Fig.2. Partial derivatives will be denoted by a comma followed by the particular coordinates as subscripts.

The circumferential stiffeners or ribs are assumed to act as slender, curved beams possessing a plane of longitudinal symmetry and undergoing only flexural and extensional deformations and radial interaction with the shell. The relevant geometrical properties of a normal cross section of a rib are then the area A and the area moment of inertia I with respect to the centroidal principal axis normal to the plane of the rib.

A representative reinforced circular penetration or ring intersecting the shell is shown in Fig.3 in the transverse plane of intersection normal to the axis of the shell. The ring is assumed to resist flexural, extensional, and torsional deformations. A normal cross section of the ring has an area $\bar{A}$ with an axis of symmetry 2-2 in the plane of the ring. The axis 1-1 is the other centroidal principal axis of the cross section, located a distance $\bar{\rho}$ from the transverse axis of the shell. The area moments of inertia of the cross section with respect to the 1-1 and 2-2 axes are denoted by I_1 and I_2, respectively. The distance e from the axis 1-1 to the point of intersection of the ring and the shell is assumed to be independent of ϕ. The distance $\bar{e}$ is measured from the axis 1-1 to the point of intersection of the ring and the flat membrane covering the opening. The vertical distance from the plane of the ring to points above it on the shell middle surface at $\rho = \rho_0$ is denoted by $h(\phi)$, and the depth of the ring, by h_1.

The materials of the shell, ribs, and ring, assumed different in the analysis, are homogeneous, isotropic, and elastic. The material constants are the Young's moduli E, E', and $\bar{E}$, and Poisson's ratios ν, ν', and $\bar{\nu}$ for the shell, rib, and ring, respectively. The torsional rigidity of the ring depends on $\bar{E}$, $\bar{\nu}$, and the geometry of the cross section, and is denoted by C.

The solution for the total state of deformation of the shell is obtained by superposing the intermediate solutions for (a) a long, unstiffened, and unperforated circular cylindrical thin shell, closed at the ends, under external hydrostatic pressure, (b) a long, unstiffened, and unperforated circular cylindrical thin shell under a prescribed number of arbitrary radial line loads, such as those exerted by the ribs, and (c) a long, unstiffened, circular cylindrical shallow thin shell under arbitrary loading along the boundary of a circular penetration. Quantities referring to these intermediate solutions (a), (b), and (c) are denoted by the subscripts a, b, and c, respectively. Shell quantities without such subscripts refer to the solution for the total state of deformation evaluated, in general, by summing results from cases (a), (b), and (c) above. This total solution for the shell must fulfill specified boundary conditions along the ribs and the reinforced penetration. For instance, the loads exerted by the shell on the ring are shown in Fig.3 where $\tilde{Q}_\rho$ and $\tilde{N}_{\rho\phi}$ are respectively the effective transverse and membrane shear stress resultants defined, in general, as

$$\tilde{Q}_\rho \equiv Q_\rho - \rho^{-1} M_{\rho\phi,\phi} , \quad \tilde{N}_{\rho\phi} \equiv N_{\rho\phi} + R^{-1} M_{\rho\phi} \cos^2 \phi , \tag{2}$$

with

$$Q_\rho = M_{\rho,\rho} + \rho^{-1} (M_\rho - M_\phi + M_{\phi\rho,\phi}) . \tag{3}$$

The final form of the solution is expressed in terms of Fourier series expansions in the θ or ϕ coordinates, with coefficients that are functions of the η or ρ coordinates, respectively, and contain arbitrary integration constants and various constant parameters. During the computation, the different series are truncated and the method of least squares is employed in solving for the appropriate number of integration constants from the boundary conditions. Convergence is verified numerically.

The numerical data reported here refer to the state of stress in an unstiffened and a rib-stiffened cylindrical shell, respectively, in the presence of a reinforced circular penetration. The results are also utilized in calculating the state of stress concentration in the shell. For this purpose, a dimensionless principal stress concentration factor $\bar{N}$ is defined, in general, as

$$\bar{N} \equiv \max | \sigma_1, \sigma_2 | / \max | \bar{\sigma}_1, \bar{\sigma}_2 | , \tag{4}$$

where σ_1, σ_2 are the principal stresses at a point of the shell with the ribs and the penetration present, while $\bar{\sigma}_1$, $\bar{\sigma}_2$ are the principal stresses at the same point in the absence of the ribs and the penetration. The former are given by

$$2\sigma_{1,2} = \sigma_\rho + \sigma_\phi \pm [(\sigma_\rho - \sigma_\phi)^2 + 4\,\tau_{\rho\phi}^2\,]^{\frac{1}{2}} \quad , \qquad (5)$$

in terms of the normal and shearing stresses σ_ρ, σ_ϕ, and $\tau_{\rho\phi}$, respectively, in the ρ, ϕ coordinate system, while the latter, for the loading considered here, correspond to

$$\max \mid \bar{\sigma}_1, \bar{\sigma}_2 \mid = pR/t \quad . \qquad (6)$$

Denoting by z the thickness coordinate of the shell, measured positive outward from the middle surface, with

$$\left.\begin{aligned} \bar{N}_\rho &\equiv \sigma_\rho t = N_\rho - 12zM_\rho/t^2 \quad , \\ \bar{N}_\phi &\equiv \sigma_\phi t = N_\phi - 12zM_\phi/t^2 , \\ \bar{N}_{\rho\phi} &\equiv \tau_{\rho\phi} t = N_{\rho\phi} + 12zM_{\rho\phi}/t^2 \quad , \end{aligned}\right\} \qquad (7)$$

it follows from Eqs.(4)-(6) that

$$\bar{N} = (2pR)^{-1} \max \mid \bar{N}_\rho + \bar{N}_\phi \pm [(\bar{N}_\rho - \bar{N}_\phi)^2 + 4\bar{N}_{\rho\phi}^2\,]^{\frac{1}{2}} \mid \quad . \qquad (8)$$

From Eq.(8), setting z equal to $\frac{1}{2}t$, $-\frac{1}{2}t$, and zero in Eq.(7), the particular values of $\bar{N}$ at the outer, inner, and middle surfaces of the shell, respectively, are determined.

2. CLOSED CYLINDRICAL SHELL UNDER HYDROSTATIC PRESSURE

For a long, unstiffened, and unperforated circular cylindrical thin shell, closed at the ends, under external hydrostatic pressure, the solution is[6]

$$\left. \begin{aligned} & N_{a\eta} = \tfrac{1}{2}pR, \; N_{a\theta} = -pR, \quad U_a = (\nu - \tfrac{1}{2})\; pR^2(Et)^{-1}\eta \quad , \\ & W_a = \tfrac{1}{2}(\nu - 2)\; pR^2(Et)^{-1} \end{aligned} \right\} \quad (9)$$

in the η, θ coordinate system, and

$$\left. \begin{aligned} & N_{a\rho} = \tfrac{1}{4}pR\;(\cos 2\phi - 3) \quad , \quad N_{a\phi} = -\tfrac{1}{4}pR\;(3 + \cos 2\phi) \quad , \\ & N_{a\rho\phi} = N_{a\phi\rho} = -\tfrac{1}{4}pR \sin 2\phi \quad , \\ & U_{a\rho} = (\nu - \tfrac{1}{2}) \quad pR(Et)^{-1}\rho \cos^2 \phi \; , \\ & U_{a\phi} = \tfrac{1}{2}(\tfrac{1}{2} - \nu) \quad pR(Et)^{-1}\rho \sin 2\phi \quad , \\ & W_a = \tfrac{1}{2}(\nu - 2)\; pR^2\; (Et)^{-1} \end{aligned} \right\} \quad (10)$$

in the ρ, ϕ coordinate system, all other quantities being equal to zero, so that from Eqs.(2) and (3),

$$\bar{Q}_{a\rho} = 0, \quad \bar{N}_{a\rho\phi} = N_{a\rho\phi}. \qquad (11)$$

3. CYLINDRICAL SHELL UNDER MULTIPLE ARBITRARY RADIAL LINE LOADS

For a long, unstiffened, and unperforated circular cylindrical thin shell under an arbitrary radial load, the governing displacement equations of equilibrium are [13]

$$\left. \begin{aligned} & U_{b,\eta\eta} + \tfrac{1}{2}(1 - \nu)\; U_{b,\theta\theta} + \tfrac{1}{2}(1 + \nu)\; V_{b,\theta\eta} + \nu W_{b,\eta} \\ & + \kappa[\tfrac{1}{2}(1 - \nu)\; U_{b,\theta\theta} - W_{b,\eta\eta\eta} + \tfrac{1}{2}(1 - \nu)\; W_{b,\eta\theta\theta}] = 0 \quad , \\ & \tfrac{1}{2}(1 + \nu)\; U_{b,\eta\theta} + V_{b,\theta\theta} + \tfrac{1}{2}(1 - \nu)\; V_{b,\eta\eta} + W_{b,\theta} \\ & + \kappa[\tfrac{3}{2}(1 - \nu)\; V_{b,\eta\eta} - \tfrac{1}{2}(3 - \nu)\; W_{b,\eta\eta\theta}] = 0 \quad , \end{aligned} \right\} \quad (12)$$

$$\left.\begin{aligned}
&\nu U_{b,\eta} + V_{b,\theta} + W_b + \kappa[\tfrac{1}{2}(1-\nu)\, U_{b,\eta\theta\theta} - U_{b,\eta\eta\eta} \\
&- \tfrac{1}{2}(3-\nu)\, V_{b,\eta\eta\theta} + W_{b,\theta\theta\theta\theta} + 2W_{b,\eta\eta\theta\theta} + W_{b,\eta\eta\eta\eta} \\
&+ 2W_{b,\theta\theta} + W_b] = p'R^2/D \quad , \\
&\qquad \kappa \equiv K/DR^2 \quad ,
\end{aligned}\right\}$$

where

$$D \equiv Et/(1-\nu^2) \quad , \quad K \equiv Et^3/12(1-\nu^2) \quad , \tag{13}$$

are respectively the extensional and flexural rigidities of the shell.

In the particular case of an arbitrary radial line load, solutions of Eq.(12) decaying to zero as $\eta \to \pm\infty$ are sought. Expanding the line load exerted on the shell by a single rib located at $\eta = 0$, and the displacements in Eq.(12), in terms of suitable Fourier series in θ,

$$\left.\begin{aligned}
&\{p', U_b, W_b\} = \sum_{m=0}^{\infty} \{p_m\delta(\eta), U_m(\eta), W_m(\eta)\} \cos m\theta \quad , \\
&V_b = \sum_{m=0}^{\infty} V_m(\eta) \sin m\theta \quad ,
\end{aligned}\right\} \tag{14}$$

where m is an integer, p_m are arbitrary constants denoting interaction load amplitudes, $\delta(\eta)$ is the Dirac delta function, and U_m, V_m, W_m are displacement amplitudes, and applying to Eq.(12) the Fourier transform defined, for an arbitrary function $f(\eta)$, as

$$\bar{f}(\alpha) = (2\pi)^{-\frac{1}{2}} \int_{-\infty}^{\infty} f(\eta) \exp i\alpha\eta \, d\eta \quad , \tag{15}$$

where α is the transform variable corresponding to η, and $i \equiv (-1)^{\frac{1}{2}}$, a system of equations for $\bar{U}_m(\alpha)$, $\bar{V}_m(\alpha)$, and $\bar{W}_m(\alpha)$ is obtained the solution of which is[6] of the form

$$\{\bar{U}_m, \bar{V}_m, \bar{W}_m\} = p_m R\{f_1, f_2, f_3\}/(2\pi)^{\frac{1}{2}} D\Delta \quad , \tag{16}$$

where

$$\left.\begin{aligned}
\Delta(\alpha) &\equiv a_5\,(\alpha^8 + a_4\alpha^6 + a_3\alpha^4 + a_2\alpha^2 + a_1) \quad ,\\
f_1(\alpha) &\equiv i\alpha(b_1\alpha^4 + b_2\alpha^2 + b_3) \quad ,\\
f_2(\alpha) &\equiv b_4\alpha^4 + b_5\alpha^2 + b_6 \quad ,\\
f_3(\alpha) &\equiv b_7\alpha^4 + b_8\alpha^2 + b_9 \quad ,
\end{aligned}\right\} \qquad (17)$$

and the coefficients a_i, $i = 1, 2, \ldots, 5$, and b_i, $i = 1, 2, \ldots, 9$, depend on ν, κ, m. It should be noted that $p_1 \equiv 0$ if the equilibrium of the forces exerted on the rib by the shell is to be ensured. Accordingly, solutions obtained in this section are for $m \neq 1$.

In order to determine U_m, V_m, W_m, the inverse Fourier transform, defined as

$$f(\eta) = (2\pi)^{-\frac{1}{2}}\int_{-\infty}^{\infty} [\bar{f}(\alpha)/\exp i\alpha\eta]\, d\alpha \quad , \qquad (18)$$

is applied to Eq.(16), the resulting integrals being evaluated by means of contour integration in the lower half of the complex plane, taking account of the fact that U_b is an odd function of η while V_b and W_b are even functions. Since Δ is a fourth order polynomial in α^2 with real coefficients, it can be written as

$$\Delta = a_5\,[\alpha^4 - (a_m^{(1)2} + a_m^{(3)2})\alpha^2 + a_m^{(1)2}a_m^{(3)2}]\,[\alpha^4 - (a_m^{(2)2} + a_m^{(4)2})\alpha^2 + a_m^{(2)2}a_m^{(4)2}] \quad , \qquad (19)$$

where $a_m^{(s)2}$, $s = 1, 2, 3, 4$, are the roots of the polynomial, such that

$$\bar{a}_m^{(3)} = -a_m^{(1)} \ , \quad \bar{a}_m^{(4)} = -a_m^{(2)} \quad , \qquad (20)$$

with a superposed bar denoting the complex conjugate, if $a_m^{(3)}$, $a_m^{(4)}$ and $a_m^{(1)}$, $a_m^{(2)}$ are respectively in the third and fourth quadrants of the complex plane.

For $m \geq 2$, it follows that

$$\left.\begin{aligned}\{U_m, V_m, W_m\} = 2p_m RD^{-1} \sum_{s=1}^{2} \underline{Re}\ [\{sgn(\eta)\ Q_{U_m}^{(s)},\\ -Q_{V_m}^{(s)}, -Q_{W_m}^{(s)}\}\exp \xi],\ \xi \equiv -ia_m^{(s)}|\eta|,\end{aligned}\right\} \quad (21)$$

where $\underline{Re}$ denotes the real part, and

$$\{Q_{U_m}^{(s)}, Q_{V_m}^{(s)}, Q_{W_m}^{(s)}\} \equiv \lim_{\alpha \to a_m^{(s)}} \{-f_1, f_2, f_3\}\ i(\alpha - a_m^{(s)})/\Delta \quad (22)$$

are the appropriate residues at a simple pole, the numerically evaluated roots of Δ, for the corresponding range of m employed in the calculations, having been found to be distinct and different from the roots of f_1, f_2, and f_3.

For $m = 0$, f_2/Δ vanishes, therefore, $V_0 = 0$. At the origin of the complex plane, where Δ now has a double root denoted by $a_0^{(2)}$, f_1/Δ has a simple pole, while f_3/Δ is analytic, so that

$$Q_{U_0}^{(2)} = \frac{1}{2}\nu/(\nu^2 - \kappa - 1), \quad Q_{W_0}^{(2)} = 0. \quad (23)$$

Furthermore, in the lower half of the complex plane, Δ has the remaining two distinct roots $a_0^{(1)}$ and $a_0^{(3)}$, different from those of f_1 and f_3, and the corresponding residues can be evaluated from Eq.(22) with $m = 0$. Then, U_0 and W_0 are determined from Eq.(21) with $m = 0$.

Finally, considering a given number N of pairs of arbitrary radial line loads located symmetrically across the transverse axis of the shell at $\eta = \pm \ell_j/R$, $j = 1, 2, \ldots, N$, where ℓ_j represents half the distance between the j-th pair of ribs, the solution for the displacements is

$$\left.\begin{aligned}
U_b &= 2RD^{-1}\sum_{j=1}^{N}\sum_{\substack{m=0\\m\neq 1}}^{\infty}\sum_{s=1}^{2}\underline{\underline{Re}}[Q_{U_m}^{(s)}(\text{sgn}\ \eta_j'\ \exp\ \xi_j' \\
&\qquad + \text{sgn}\ \eta_j''\ \exp\ \xi_j'')]\ p_{mj}\cos m\theta, \\
V_b &= -2RD^{-1}\sum_{j=1}^{N}\sum_{\substack{m=0\\m\neq 1}}^{\infty}\sum_{s=1}^{2}\underline{\underline{Re}}[Q_{V_m}^{(s)}(\exp\ \xi_j' \\
&\qquad + \exp\ \xi_j'')]\ p_{mj}\sin m\theta, \\
W_b &= -2RD^{-1}\sum_{j=1}^{N}\sum_{\substack{m=0\\m\neq 1}}^{\infty}\sum_{s=1}^{2}\underline{\underline{Re}}[Q_{W_m}^{(s)}(\exp\ \xi_j' \\
&\qquad + \exp\ \xi_j'')]\ p_{mj}\cos m\theta, \\
\xi_j' &\equiv -ia_m^{(s)}|\eta_j'|\ , \qquad \xi_j'' \equiv -ia_m^{(s)}|\eta_j''|, \\
\eta_j' &\equiv \eta - \ell_j/R\ , \qquad \eta_j'' \equiv \eta + \ell_j/R\ ,
\end{aligned}\right\} \quad (24)$$

where p_{mj} are interaction load amplitudes for the j-th pair of radial line loads. This solution allows non-uniform spacing of adjacent ribs.

Substituting Eq.(24) into the following resultant stress-displacement relations[13]

$$\begin{aligned}
N_{b\eta} &= DR^{-1}\ [U_{b,\eta} + \nu(W_b + V_{b,\theta}) - \kappa W_{b,\eta\eta}]\ , \\
N_{b\theta} &= DR^{-1}\ [W_b + V_{b,\theta} + \nu U_{b,\eta} + \kappa(W_b + W_{b,\theta\theta})], \\
N_{b\eta\theta} &= \tfrac{1}{2}(1-\nu)DR^{-1}[U_{b,\theta} + V_{b,\eta} + \kappa(V_{b,\eta} - W_{b,\eta\theta})], \\
N_{b\theta\eta} &= \tfrac{1}{2}(1-\nu)DR^{-1}[U_{b,\theta} + V_{b,\eta} + \kappa(U_{b,\theta} + W_{b,\eta\theta})],
\end{aligned}$$

$$
\left.\begin{aligned}
M_{bn} &= \kappa D[W_{b,nn} - U_{b,n} + \nu(W_{b,\theta\theta} - V_{b,\theta})],\\
M_{b\theta} &= \kappa D(W_b + W_{b,\theta\theta} + \nu W_{b,nn}),\\
M_{bn\theta} &= (1-\nu)\kappa D(V_{b,n} - W_{b,n\theta}),\\
M_{b\theta n} &= \tfrac{1}{2}(1-\nu)\kappa D(U_{b,\theta} - V_{b,n} + 2W_{b,n\theta}),
\end{aligned}\right\} \quad (25)
$$

the corresponding solution for the stress and couple resultants is obtained. These results are then represented in the ρ,ϕ coordinate system by transformation,[6] after which, expressions for $\tilde{Q}_{b\rho}$ and $\tilde{N}_{b\rho\phi}$ are found from Eqs.(2) and (3).

4. CYLINDRICAL SHELL UNDER ARBITRARY LOADING ALONG A CIRCULAR PENETRATION

For a long, unstiffened, circular cylindrical shallow thin shell under edge loading only, the stress and couple resultants can be expressed[2] in terms of a complex, dimensionless potential function ψ as

$$
\left.\begin{aligned}
N_{c\rho} &= B\rho^{-2}\underline{\mathrm{Im}}(\psi,_{\phi\phi} + \rho\psi,_{\rho}), \quad N_{c\phi} = B\underline{\mathrm{Im}}(\psi,_{\rho\rho}),\\
N_{c\rho\phi} &= N_{c\phi\rho} = B\rho^{-2}\underline{\mathrm{Im}}(\psi,_{\phi} - \rho\psi,_{\rho\phi}),\\
M_{c\rho} &= -K\rho_o\underline{\mathrm{Re}}[\psi,_{\rho\rho} + \nu\rho^{-2}(\psi,_{\phi\phi} + \rho\psi,_{\rho})],\\
M_{c\phi} &= -K\rho_o\underline{\mathrm{Re}}[\nu\psi,_{\rho\rho} + \rho^{-2}(\psi,_{\phi\phi} + \rho\psi,_{\rho})],\\
M_{c\rho\phi} &= -M_{c\phi\rho} = (1-\nu)K\rho_o\rho^{-2}\underline{\mathrm{Re}}(\rho\psi,_{\rho\phi} - \psi,_{\phi}),\\
B &\equiv \rho_o Et^2/[12(1-\nu^2)]^{\frac{1}{2}},
\end{aligned}\right\} \quad (26)
$$

where Im denotes the imaginary part, and

$$\left.\begin{aligned} &\nabla^2\nabla^2\phi + 8i\beta^2R^2\phi_{,\eta\eta} = 0, \ \mathrm{Re}(\phi) \equiv -W_c/\rho_o, \\ &\nabla^2(\ ) \equiv (\ )_{,\eta\eta} + (\ )_{,\theta\theta}, \ \beta^2 \equiv \tfrac{1}{4}[3(1-\nu^2)]^{\frac{1}{2}}/Rt, \end{aligned}\right\} \quad (27)$$

with β as the material-curvature parameter. Various conditions concerning the applicability of the shallow shell theory to the present problem have been recorded elsewhere.[1]

The solution of Eq.(27) in the ρ,ϕ coordinate system, satisfying the conditions of biaxial symmetry and of decaying to zero as $\rho \to \infty$, is[6]

$$\left.\begin{aligned} &\phi = D^{-1}\sum_{n=0}^{\infty}\sum_{m=0}^{\infty}(A_m + iA_m')\lambda_{nm0}\cos 2n\phi, \\ &\lambda_{nm\ell} \equiv (i)^{2n+m}[J_{m-2n} + (1-\delta_{n0})J_{m+2n}]H_{m+\ell}^{(1)}, \end{aligned}\right\} \quad (28)$$

where n,ℓ are integers, δ_{n0} is a Kronecker delta, A_m, A_m' are arbitrary integration constants, and J_k and $H_k^{(1)}$ are the Bessel and Hankel functions of the first kind and integer order k, respectively, of the complex, dimensionless argument $\beta\rho(2i)^{\frac{1}{2}}$; these functions are evaluated by means of a series representation. Expressions for $\bar{Q}_{c\rho}$ and $\hat{N}_{c\rho\phi}$ are found from Eqs. (2) and (3) by employing Eqs.(26) and (28).

In order to determine $U_{c\rho}$ and $U_{c\phi}$, with W_c given by Eq.(27), the following resultant stress-displacement relations[3]

$$\left.\begin{aligned} &U_{c\rho,\rho} = (Et)^{-1}(N_{c\rho} - \nu N_{c\phi}) - W_cR^{-1}\sin^2\phi, \\ &\rho^{-1}(U_{c\rho} + U_{c\phi,\phi}) = (Et)^{-1}(N_{c\phi} - \nu N_{c\rho}) - W_cR^{-1}\cos^2\phi, \\ &\rho^{-1}(U_{c\rho,\phi} - U_{c\phi}) + U_{c\phi,\rho} = 2(1+\nu)(Et)^{-1}N_{c\rho\phi} - W_cR^{-1}\sin 2\phi, \end{aligned}\right\} \quad (29)$$

are utilized, the solutions being subject to conditions of symmetry specified above.

Finally, W_c in the η,θ coordinate system is[6]

$$W_c = RD^{-1} \sum_{m=0}^{\infty} \sum_{n=0}^{\infty} (C'_{mn} A'_n - C_{mn} A_n) \cos m\theta, \tag{30}$$

where

$$\left.\begin{aligned} C_{mn}(\eta) + iC'_{mn}(\eta) &\equiv \rho_0 R^{-1} D_{mn} \cos [\beta \eta R (2i)^{\frac{1}{2}} - \tfrac{1}{2} n\pi] \exp \tfrac{1}{2} i n \pi, \\ D_{mn}(\eta) &\equiv \begin{Bmatrix} (\pi)^{-1} \\ (2\pi)^{-1} \end{Bmatrix} \int_{-\pi}^{\pi} H_n^{(1)} \cos n\phi \cos m\theta \, d\theta \text{ if } \begin{Bmatrix} m \neq 0 \\ m = 0 \end{Bmatrix}, \end{aligned}\right\} \tag{31}$$

noting the transformation relations in Eq.(1); the integral appearing in Eq.(31) is evaluated numerically.

5. BOUNDARY CONDITIONS

Considering first the boundary conditions at the ribs, since the total solution is symmetric in η, only the conditions at $\eta = \ell_i/R$, $i = 1, 2, \ldots, N$, namely,

$$W = w' , \tag{32}$$

need to be employed, where[13]

$$w' = c_{1i} \cos \theta + R'^4 (E'I)^{-1} \sum_{\substack{m=0 \\ m \neq 1}}^{\infty} [(1 - I/AR'^2)\delta_{m0}$$

$$-(m^2 - 1)^{-2}] p_{mi} \cos m\theta \tag{33}$$

is the outward radial displacement of the i-th pair of ribs, with c_{1i} denoting arbitrary integration constants representing rigid body displacements. From Eqs.(9),(24),(30), (32), and (33), it follows[7] that, for $m \neq 1$,

$$p_{mj} = \sum_{i=1}^{N} [\tfrac{1}{2}(\nu - 2)(1 - \nu^2)^{-1} pR\delta_{m0} + \sum_{n=0}^{\infty} (C'_{mni} A'_n - C_{mni} A_n)] B^{-1}_{mji}, \tag{34}$$

where B^{-1}_{mji} is the inverse of

$$B_{mji} \equiv 2 \sum_{s=1}^{2} \underline{\text{Re}} [Q_{W_m}^{(s)} (\exp \xi'_{ji} + \exp \xi''_{ji})]$$

$$+ (DR'^4/E'IR)[(1 - I/AR'^2)\delta_{m0} - (m^2 - 1)^{-2}]\delta_{ji} , \tag{35}$$

and C_{mni}, C'_{mni}, ξ'_{ji}, and ξ''_{ji} denote C_{mn}, C'_{mn}, ξ'_j, and ξ''_j, respectively, evaluated at $\eta = \ell_i/R$, and, for $m = 1$,

$$c_{1i} = RD^{-1}\sum_{n=0}^{\infty}(C'_{1ni}A'_n - C_{1ni}A_n). \tag{36}$$

Considering next the reinforced penetration, the loads exerted on the ring by the hydrostatic pressure and, along its external and internal boundaries, by the shell and the membrane covering the opening, are equipollent to the following system[8] of radial, tangential, and transverse forces, F_1, F_2, F_3, respectively, and torsional moment M acting along $\rho = \bar{\rho}$.

$$\left.\begin{aligned}
&\bar{\rho}^2\rho_o^{-1}F_1 \equiv \bar{\rho}N_\rho + e\tilde{N}_{\rho\zeta,\phi}, \quad \bar{\rho}\rho_o^{-1}F_2 \equiv \tilde{N}_{\rho\phi},\\
&\bar{\rho}^2\rho_o^{-1}F_3 \equiv \tfrac{1}{2}\rho_o\bar{\rho}p - [h(\phi)\tilde{N}_{\rho\phi}]_{,\phi} + \bar{\rho}[\bar{Q}_\rho + \rho_o R^{-1}(N_\rho \sin^2\phi\\
&\qquad + \tfrac{1}{2}\tilde{N}_{\rho\phi}\sin 2\phi)],\\
&\bar{\rho}\rho_o^{-1}M \equiv M_\rho - h(\phi)N_\rho + \tfrac{1}{2}\bar{e}(\bar{\rho} - \bar{e})^2\rho_o^{-1}p\\
&\qquad - e[\bar{Q}_\rho + \rho_o R^{-1}(N_\rho \sin^2\phi + \tfrac{1}{2}\tilde{N}_{\rho\phi}\sin 2\phi)].
\end{aligned}\right\} \tag{37}$$

The equilibrium of these forces and moment, the positive directions of which can be inferred from Eq.(37) and Fig.3, is essentially ensured, since it can be shown that the solution in Eq.(28) implies a self-equilibrating system of loads along the boundary of the penetration.

Denoting by u, v, and w the displacements, in the outward radial, tangential, and upward transverse directions, respectively, of points of the ring on $\rho = \bar{\rho}$, the boundary conditions at the penetration are[8]

$$\left.\begin{aligned}
&\bar{\rho}^4F_1 = \bar{E}\bar{I}_1(u_{,\phi\phi\phi\phi} - v_{,\phi\phi\phi}) + \bar{E}\bar{A}\bar{\rho}^2(u + v_{,\phi}),\\
&\bar{\rho}^4F_2 = \bar{E}\bar{I}_1(u_{,\phi\phi\phi} - v_{,\phi\phi}) - \bar{E}\bar{A}\bar{\rho}^2(u_{,\phi} + v_{,\phi\phi}),\\
&\bar{\rho}^3F_3 = C(\bar{\rho}^{-1}w_{,\phi\phi} - w_{,\rho\phi\phi}) - \bar{E}\bar{I}_2(w_{,\rho\phi\phi} + \bar{\rho}^{-1}w_{,\phi\phi\phi\phi}),\\
&\bar{\rho}^2M = C(\bar{\rho}^{-1}w_{,\phi\phi} - w_{,\rho\phi\phi}) + \bar{E}\bar{I}_2(w_{,\rho} + \bar{\rho}^{-1}w_{,\phi\phi}),
\end{aligned}\right\} \tag{38}$$

where, approximately[8],

$$\left.\begin{aligned} u &= U_{\rho} + h(\phi)W_{,\rho} + \rho_o R^{-1} W \sin^2 \phi \,, \\ \rho_o v &= \beta U_{\phi} + eU_{\rho,\phi} + h(\phi)W_{,\phi} + \tfrac{1}{2}\rho_o \beta R^{-1} W \sin 2\phi \,, \\ w &= W - eW_{,\rho} \,. \end{aligned}\right\} \quad (39)$$

Shell quantities appearing in Eqs.(37) and (39) are evaluated at $\rho = \rho_o$, and, in the course of the solution, $h(\phi)$ and $w_{,\rho}$ are replaced approximately by

$$h(\phi) = \bar{h} - \tfrac{1}{2}\rho_o^2 R^{-1} \sin^2 \phi, \quad \bar{h} \equiv h\,(0), \; w_{,\rho} = W_{,\rho} \,.$$

6. NUMERICAL AND EXPERIMENTAL RESULTS

The above analysis has been coded and numerical results for certain configurations within the range of applicability of the theory and for which experimental results are presently available have been generated by the use of a digital computer.

In the special case of a cylindrical shell stiffened by multiple ribs, with an unreinforced penetration, a comparison of the previous analyses[6,7] and experimental data has already been reported.[11] These analyses have also been confirmed by further numerical results[14] obtained on the basis of an energy method utilizing a finite difference representation. The following account, then, consists of similar comparisons between the results of the present analysis and those of further experiments for the remaining cases of an unstiffened shell with a reinforced penetration[12] and a rib-stiffened shell with a reinforced penetration[10], respectively, for which no such evaluations yet exist. The corresponding zone of influence of the penetration and the state of stress concentration about it are thereby delineated.

Numerical results obtained during the present investigation for the particular case of an unstiffened cylindrical shell with a reinforced circular penetration, and describing the variation of the dimensionless hoop and longitudinal stresses with ρ/ρ_o at the outer and inner surfaces of the shell for $\phi = 0$ and $\pi/2$, are indicated by the solid curves in Figs.4-7 where the experimental results[12] for the same case are shown by the dashed curves. The latter are based on photoelasticity tests performed[12] on an epoxy (Hysol 4290) shell model, with a ring of rectangular cross section and of the same material around the opening covered with a plug, loaded by internal hydrostatic pressure. The relevant dimensions for the test model are R = 5-7/8 inches, t = 1/4 inch, ρ_o = 7/8 inch, h_1 = 1/2 inch, and e = $\bar{e}$ = 1/8 inch; the ring has a fillet with a radius of 1/16 inch, the point at which it meets the shell being indicated by a vertical dash on the experimental curves. The value of $\bar{h}$ is taken as zero.

Corresponding results for the general case of a rib-stiffened cylindrical shell with a reinforced circular penetration are given in Figs.8-11 where the solid curves are obtained from the present analysis and the dashed curves represent the experimental data.[10] The latter are based on tests, similar to those mentioned above, conducted[10] on a model of the same material and dimensions, except for the presence of multiple ribs of rectangular cross section and of the same material, with adjacent ribs spaced uniformly a distance $2\ell_1$ apart, as shown in Fig.1, the additional relevant dimensions being ℓ_1 = 1-1/2 inches, t' = 5/16 inch, and e' = 1-1/8 inches, where t' and e' are the width and the depth of a rib, respectively. The calculations were carried out for the case N = 4; the centerlines of the first two ribs only are shown in Figs.8 and 9, with the width of the ribs indicated by a pair of vertical dashes on the experimental curves.

Finally, the calculated values of the principal stress concentration factor at the outer, inner, and middle surfaces of the shell, for the two cases considered here, are shown in Fig.12 for $0 \leq \phi \leq \pi/2$ and $\rho/\rho_o = 1$, with the curves a and b referring respectively to the unstiffened and the rib-stiffened cylindrical shell with a reinforced circular penetration.

7. CONCLUSION

From the preceding graphical comparisons of analytical and experimental results, it can be concluded that, in general, a satisfactory agreement exists. Complete agreement is not expected, since there are certain features of the test models causing localized perturbations, such as the fillets around the ring and the ribs, the finite width of the ribs, and the particular plug covering the penetration, that are not accounted for in the theory. It should also be noted that some of the experimental data reported for the fillet region at the ring are based on extrapolations.

It may, however, be desirable to refine the present analysis by considering the influence of the circumferential interaction between the shell and the ribs.

ACKNOWLEDGMENTS

This research was sponsored by the Structural Mechanics Laboratory of the Naval Ship Research and Development Center under Naval Ship Systems Command Subproject SF 013 0303, Task 1956, and carried out under Office of Naval Research Contract No. Nonr-4835(00)(X). Discussions held by the staff of the General Technology Corporation with Dr. O. Lomacky of the Naval Ship Research and Development Center are gratefully acknowledged. Dr. J. A. Euler, Consultant, performed the computer coding.

REFERENCES

[1]Lomacky, O., "A Summary of Submarine Structural Research. Part 1. Conventional Hull Configurations. Chapter IX. Hull Penetrations," *Research and Development Report 2309*, May 1967, Structural Mechanics Laboratory, Naval Ship Research and Development Center, Washington, D.C.

[2]Eringen, A. C., Naghdi, A. K., and Thiel, C. C., "State of Stress in a Circular Cylindrical Shell with a Circular Hole," *Welding Research Council Bulletin No. 102*, Jan. 1965, Welding Research Council of the Engineering Foundation, New York, N.Y.

[3]Eringen, A. C., Naghdi, A. K., Mahmood, S. S., Thiel, C. C., and Ariman, T., "Stress Concentrations in Two Normally Intersecting Cylindrical Shells Subject to Internal Pressure," *Welding Research Council Bulletin No. 139*, Apr. 1969, Welding Research Council of the Engineering Foundation, New York, N.Y.

[4]Maye, R. F. and Eringen, A. C., "Further Analysis of Two Normally Intersecting Cylindrical Shells Subjected to Internal Pressure," *Nuclear Engineering and Design*, Vol. 12, 1970, pp. 457-474.

[5]Parfitt, V. R., Claus, W. D., Jr., Kafadar, C. B., and Eringen, A. C., "Finite Element Stress Analysis of Thin Shells," *Technical Report No. 6-1*, Nov. 1965, General Technology Corp., West Lafayette, Ind. (AD 475 722 L).

[6]Stanisic, M. M., Euler, J. A., Dowell, E. H., and Eringen, A. C., "Stress Distribution in a Stiffened Circular Cylindrical Shell with a Circular Cutout under Hydrostatic Pressure," *Technical Report No. 7-1*, Aug. 1967, General Technology Corp., Lawrenceville, N.J. (AD 661 332).

[7]Euler, J. A. and Dowell, E. H., "Stress Distribution in a Stiffened Circular Cylindrical Shell with a Circular Cutout under Hydrostatic Pressure: Multiple Ring Stiffeners," *Technical Report No. 7-3*, Mar. 1969, General Technology Corp., Lawrenceville, N.J. (AD 852 158).

[8]Lekkerkerker, J. G. and Dowell, E. H., "Stress Distribution in a Circular Cylindrical Shell with a Circular Reinforced Cutout under External Pressure," *Technical Report No. 7-2*, Nov. 1968, General Technology Corp., Lawrenceville, N.J. (AD 849 026).

[9]Lomacky, O., "Stress Concentration Factors for Small Reinforced Circular Penetrations in Pressurized Cylindrical Shells," *Research and Development Report 2559*, Oct. 1967, Structural Mechanics Laboratory, Naval Ship Research and Development Center, Washington, D.C.

[10]Durelli, A. J., Parks, V. J., and Lee, H.-C., "Stresses in a Pressurized Ribbed Cylindrical Shell with a Reinforced Hole," Feb. 1969, Stress Analysis Laboratory, Civil Engineering and Mechanics Department, School of Engineering and Architecture, The Catholic University of America, Washington, D.C.

[11]Durelli, A. J., Parks, V. J., and Lee, H.-C., "Stresses in a Perforated Ribbed Cylindrical Shell Subjected to Internal Pressure," *International Journal of Solids and Structures*, Vol. 5, No. 6, Jun. 1969, pp. 573-586.

[12]Durelli, A. J., Parks, V. J., and Lee, H.-C., "Stresses in a Pressurized Cylindrical Shell with Two Unequal Diametrically Opposite Reinforced Circular Holes," Jul. 1968, Stress Analysis Laboratory, Civil Engineering and Mechanics Department, School of Engineering and Architecture, The Catholic University of America, Washington, D.C.

[13] Flügge, W., *Stresses in Shells*, 3rd pr., Springer-Verlag, New York, 1966, Ch. 5; App.

[14] Brogan, F. A., and Stern, P., "Analysis of Stiffened Shells with Cutouts," *LMSC-N-3N-69-1*, Aug. 1969, Lockheed Palo Alto Research Laboratory, Palo Alto, Calif.

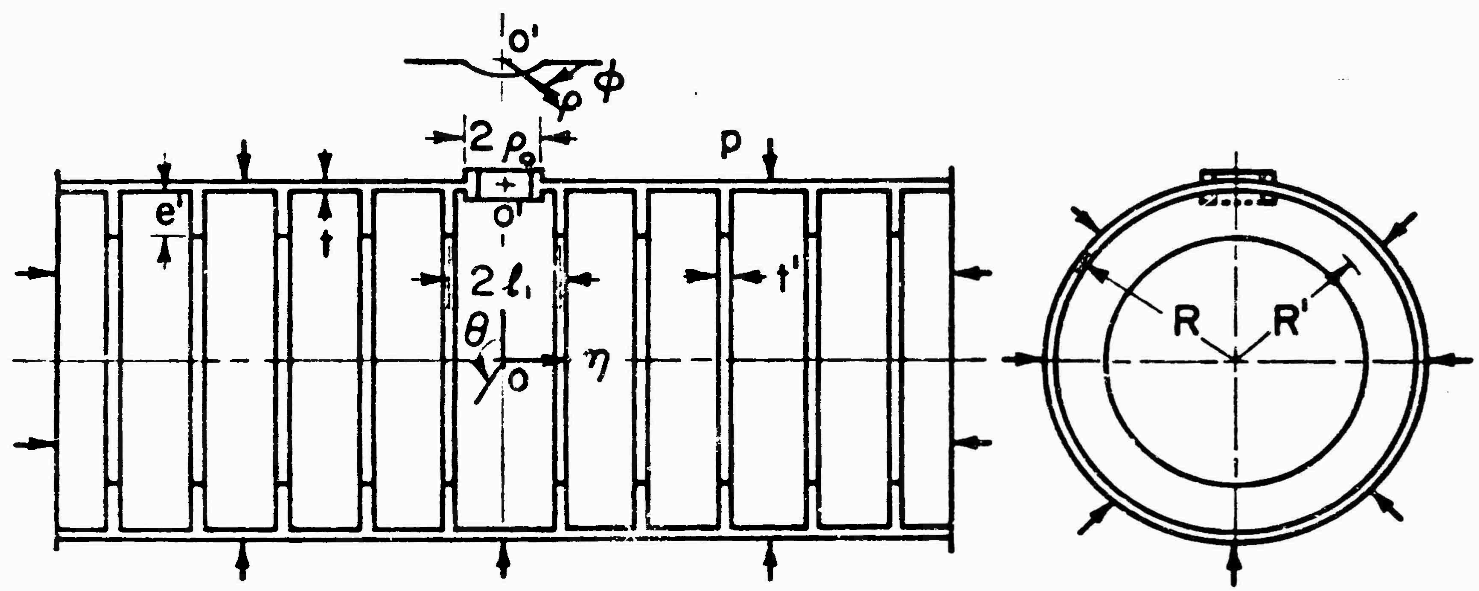

FIG. 1

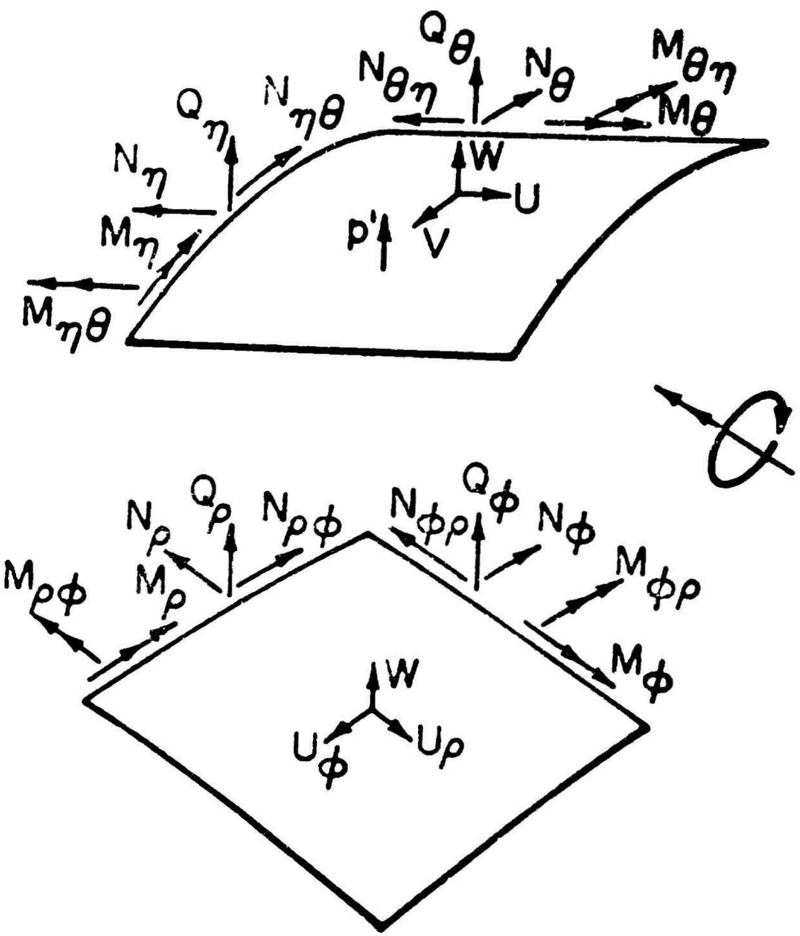

Q_θ
N_θ
$M_{\theta\eta}$
M_θ
$N_{\theta\eta}$
Q_η
$N_{\eta\theta}$
N_η
M_η
$M_{\eta\theta}$
W
U
V
p'
N_ρ
Q_ρ
$N_{\rho\phi}$
$N_{\phi\rho}$
Q_ϕ
N_ϕ
$M_{\rho\phi}$
M_ρ
$M_{\phi\rho}$
M_ϕ
W
U_ϕ
U_ρ

FIG. 2

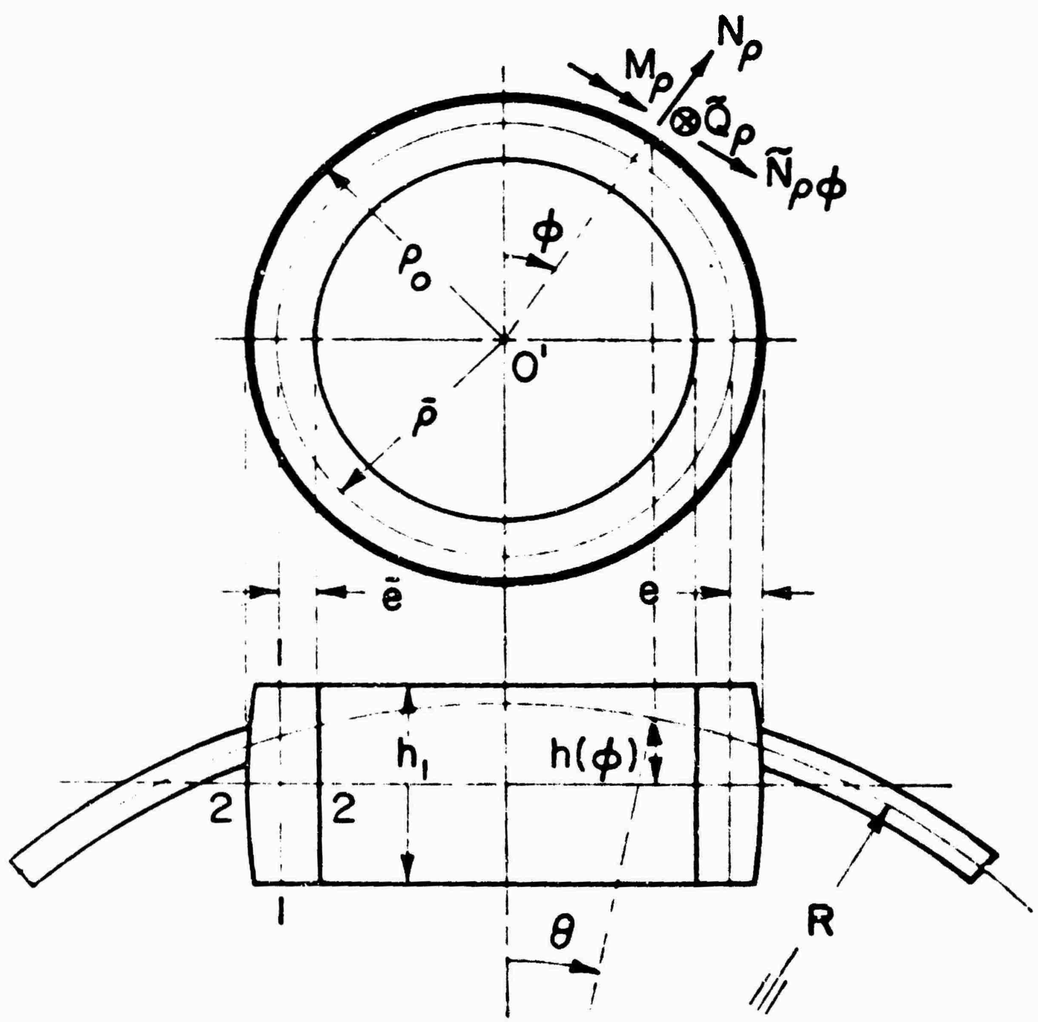

M_ρ
N_ρ
$\tilde{Q}_\rho$
$\tilde{N}_{\rho\phi}$
ϕ
ρ_o
O'
$\bar{\rho}$
$\bar{e}$
e
h_1
$h(\phi)$
2
2
1
θ
R

FIG. 3

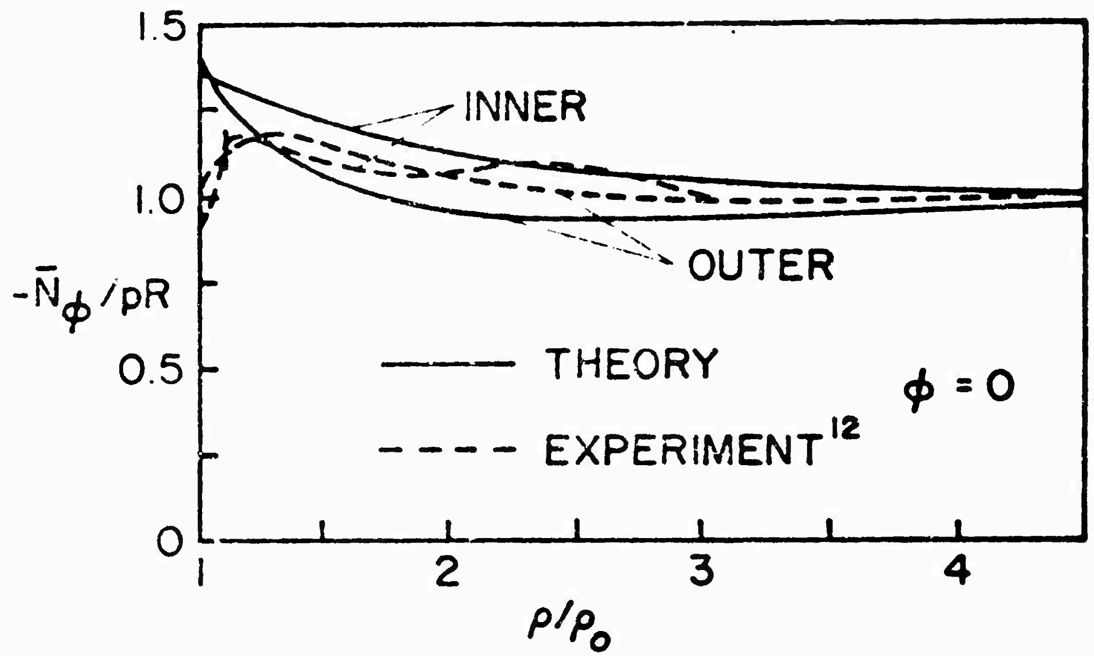
1.5
1.0
0.5
0
$-\bar{N}_\phi/pR$
INNER
OUTER
THEORY
EXPERIMENT[12]
$\phi = 0$
1
2
3
4
ρ/ρ_o

FIG. 4

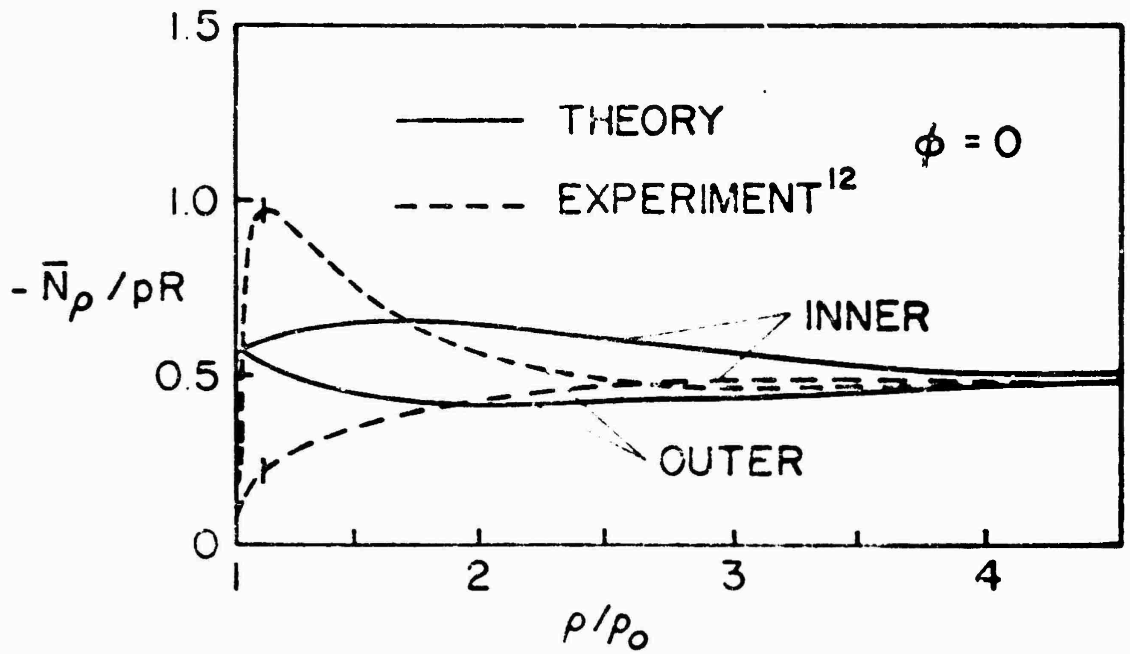
1.5
1.0
0.5
0
$-\bar{N}_\rho/pR$
THEORY
EXPERIMENT[12]
$\phi = 0$
INNER
OUTER
1
2
3
4
ρ/ρ_o

FIG. 5

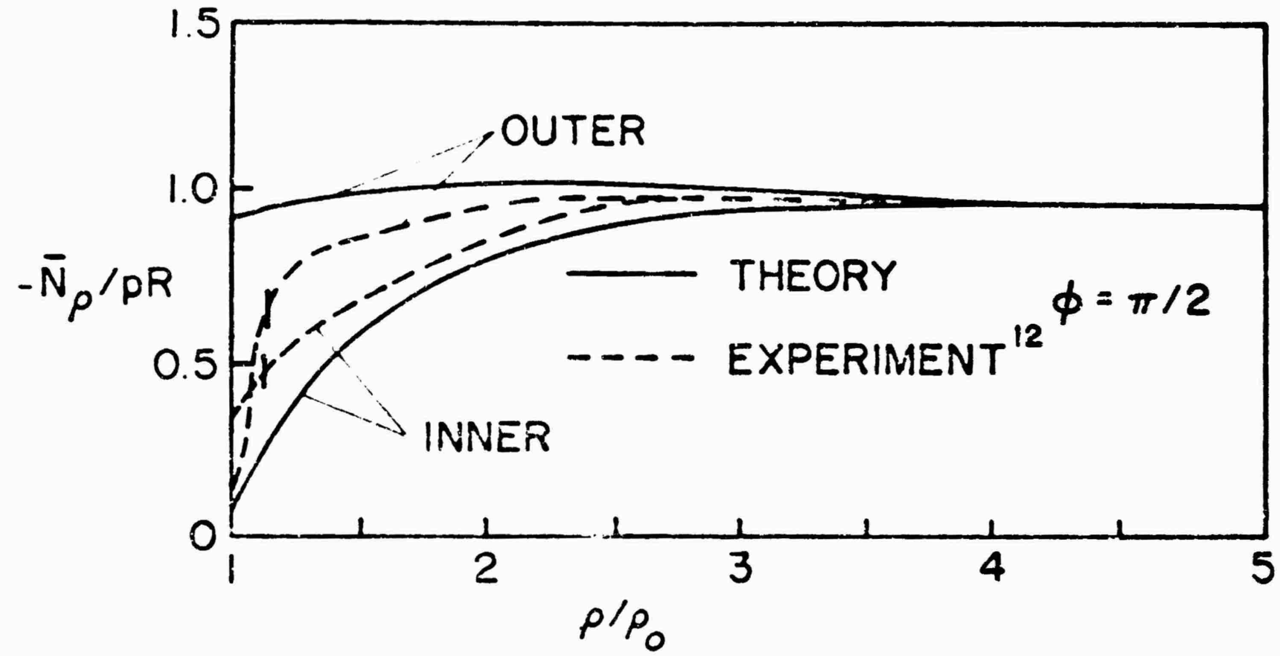
1.5
1.0
0.5
0
$-\bar{N}_\rho/pR$
OUTER
INNER
THEORY
EXPERIMENT[12]
$\phi = \pi/2$
1
2
3
4
5
ρ/ρ_o

FIG. 6

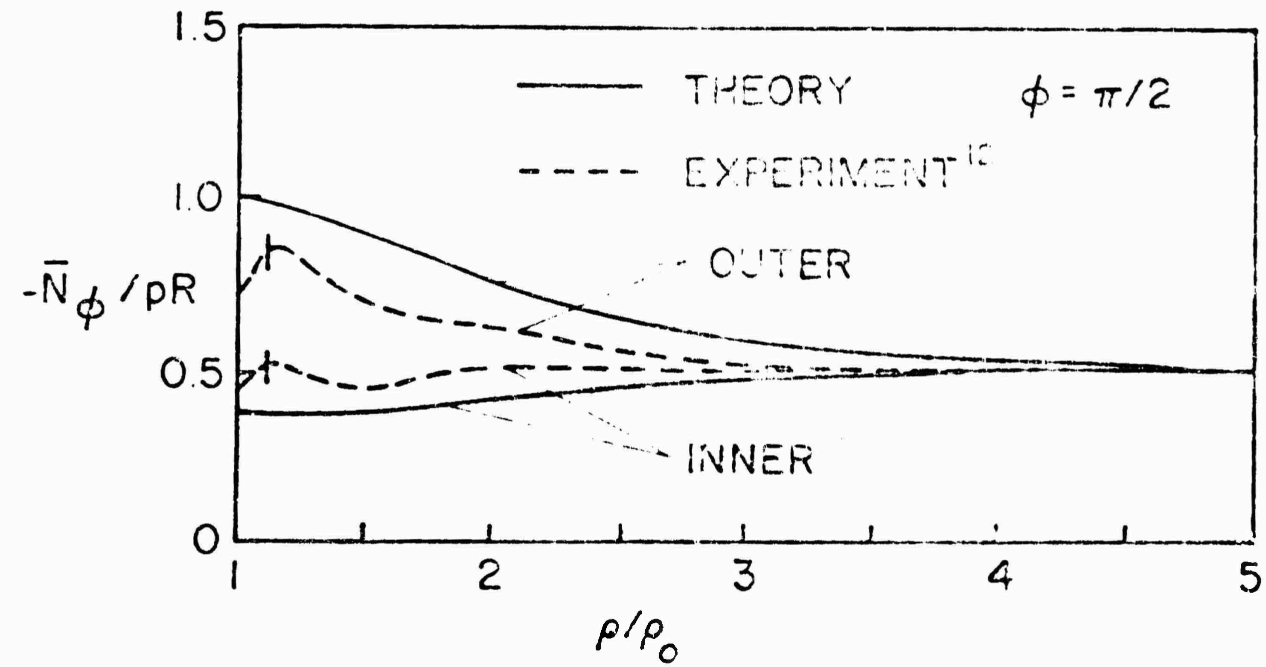
1.5
1.0
0.5
0
$-\bar{N}_\phi/pR$
THEORY
EXPERIMENT[12]
$\phi = \pi/2$
OUTER
INNER
1
2
3
4
5
ρ/ρ_o

FIG. 7

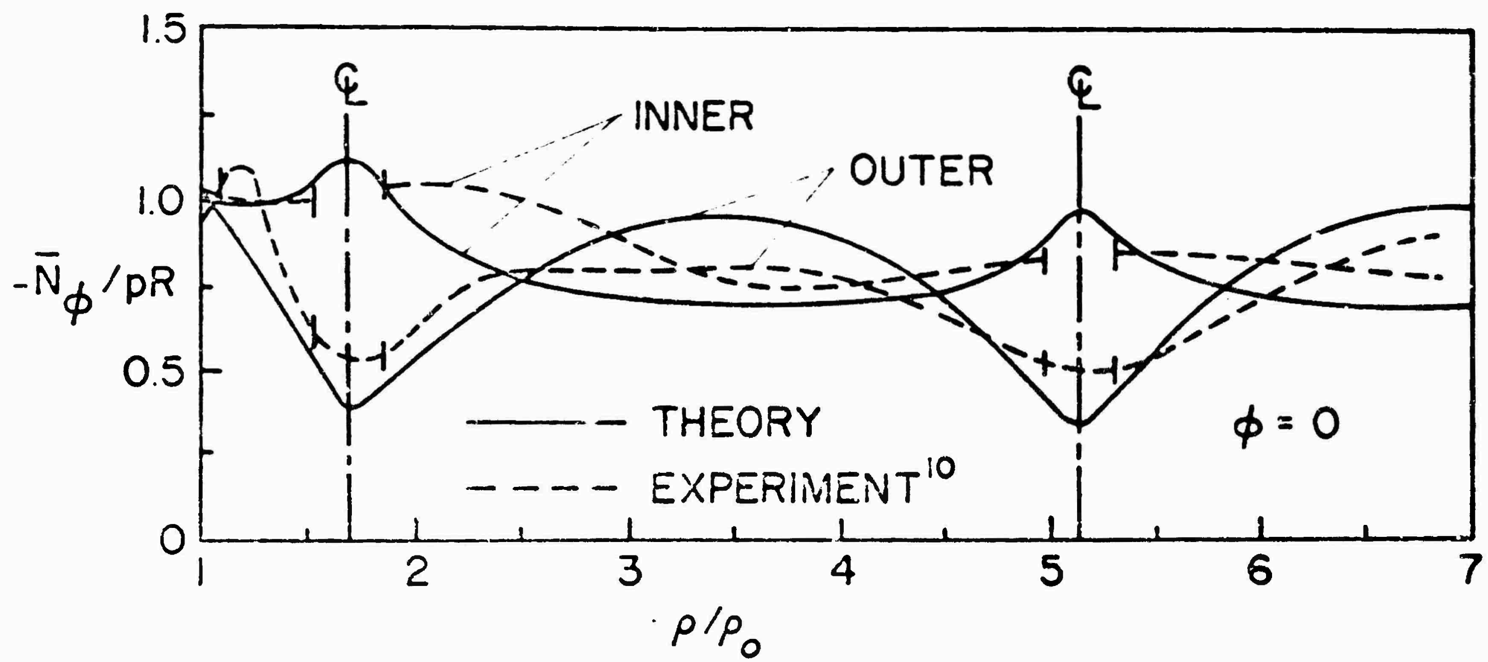
1.5
1.0
0.5
0
-N̄ϕ /pR
1
2
3
4
5
6
7
ρ/ρo
INNER
OUTER
THEORY
EXPERIMENT10
ϕ = 0

FIG. 8

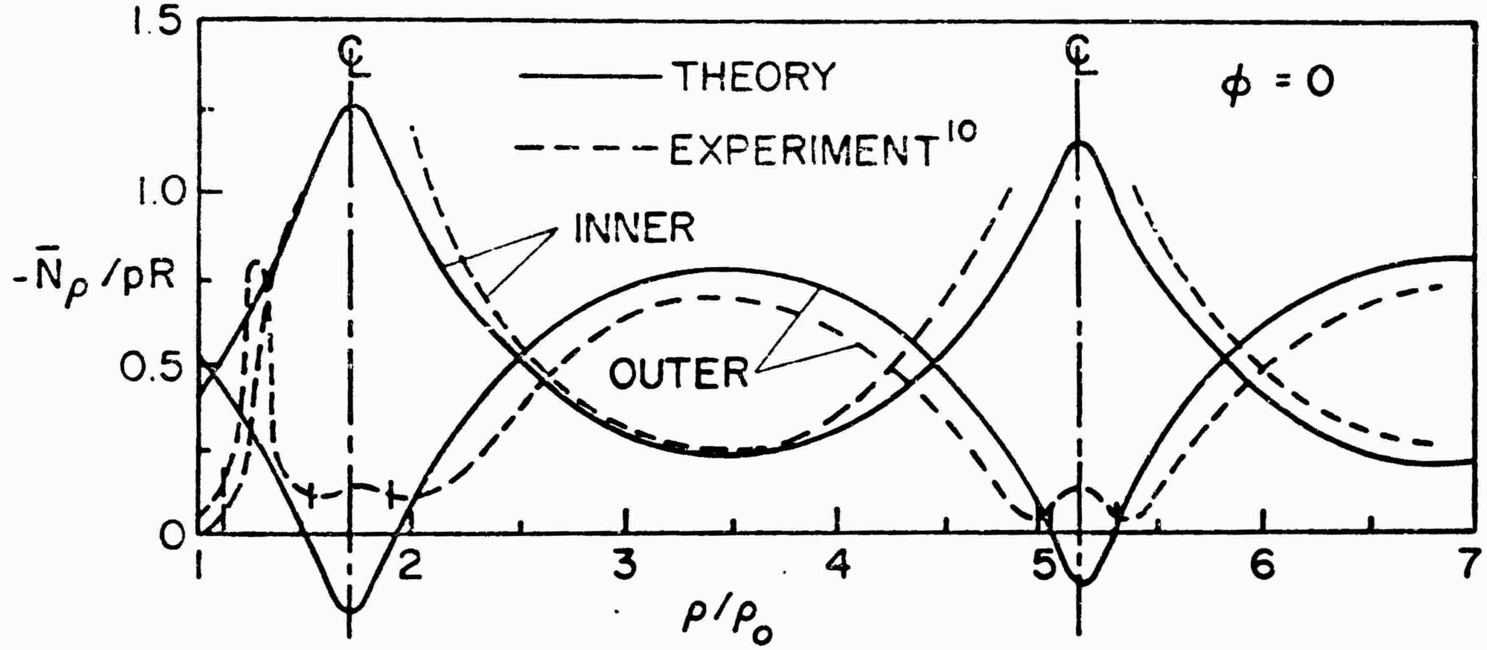
THEORY
EXPERIMENT 10
INNER
OUTER
ϕ = 0
1.5
1.0
0.5
0
-N̄ρ /pR
1
2
3
4
5
6
7
ρ/ρo

FIG. 9

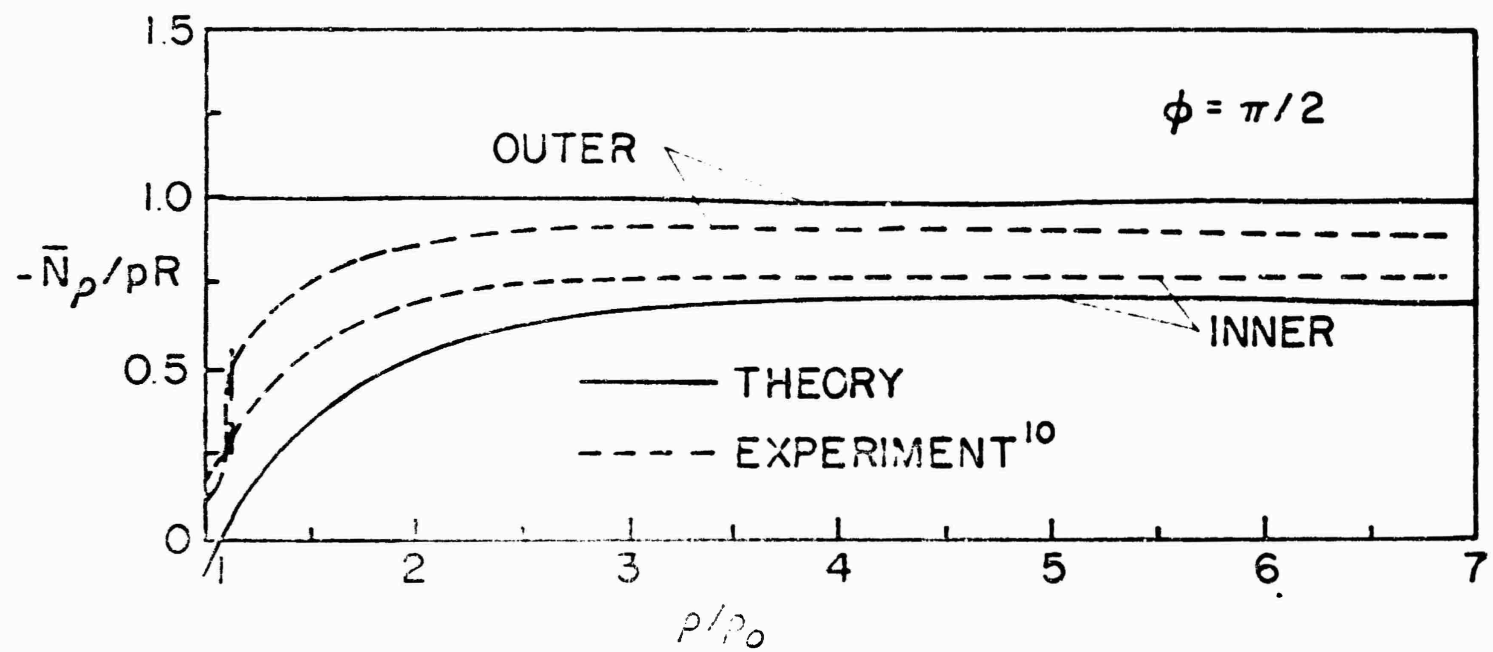
1.5
1.0
0.5
0
$-\bar{N}_\rho/pR$
1
2
3
4
5
6
7
ρ/ρ_0
$\phi = \pi/2$
OUTER
INNER
THEORY
EXPERIMENT[10]

FIG. 10

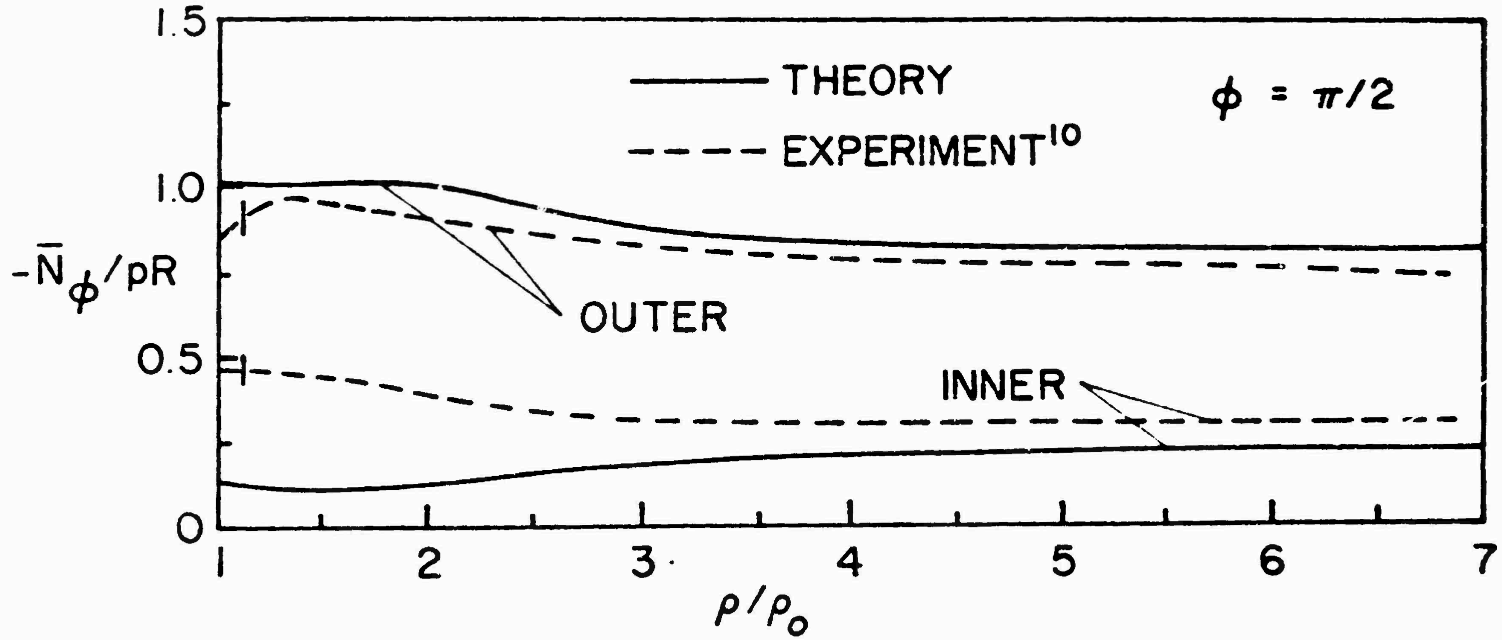
1.5
1.0
0.5
0
$-\bar{N}_\phi/pR$
THEORY
EXPERIMENT[10]
$\phi = \pi/2$
OUTER
INNER
1
2
3
4
5
6
7
ρ/ρ_o

FIG. 11

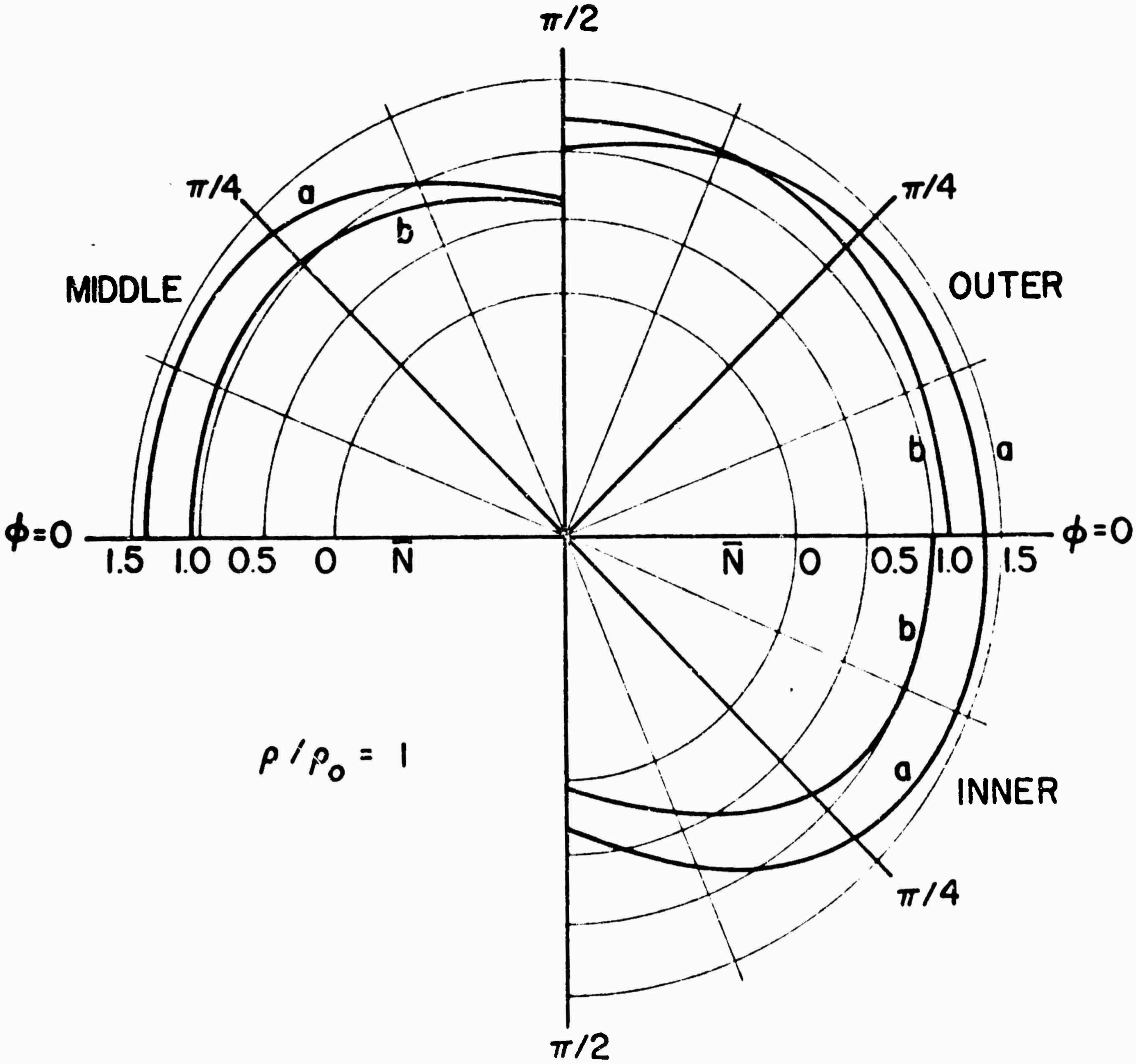
π/2
π/4
a
b
MIDDLE
OUTER
π/4
b
a
φ=0
1.5
1.0
0.5
0
N̄
N̄
0
0.5
1.0
1.5
φ=0
b
a
INNER
π/4
π/2
ρ/ρo = 1

FIG. 12

UNCLASSIFIED

Security Classification

DOCUMENT CONTROL DATA - R&D

(Security classification of title, body of abstract and indexing annotation must be entered when the overall report is classified)

1. ORIGINATING ACTIVITY (Corporate author) General Technology Corporation Lawrenceville, New Jersey 08648	2a. REPORT SECURITY CLASSIFICATION Unclassified 2b. GROUP

3. REPORT TITLE

STRUCTURAL ANALYSIS OF PRESSURE HULLS: RIB-STIFFENED CYLINDRICAL SHELL WITH REINFORCED CIRCULAR PENETRATION

4. DESCRIPTIVE NOTES (Type of report and inclusive dates)

Summary Report

5. AUTHOR(S) (Last name, first name, initial)

Richard F. Maye and Lui M. Habip

6. REPORT DATE	7a. TOTAL NO. OF PAGES	7b. NO. OF REFS
December 1969	20	14

8a. CONTRACT OR GRANT NO. Nonr-4835(00)(X) b. PROJECT NO. NSSC Subproject SF 013 0303 c. Task 1956 d.	9a. ORIGINATOR'S REPORT NUMBER(S) 7-4 9b. OTHER REPORT NO(S) (Any other numbers that may be assigned this report)

10. AVAILABILITY/LIMITATION NOTICES

THIS DOCUMENT HAS BEEN APPROVED FOR PUBLIC RELEASE AND SALE; ITS DISTRIBUTION IS UNLIMITED.

11. SUPPLEMENTARY NOTES	12. SPONSORING MILITARY ACTIVITY Naval Ship Research & Development Center Department of the Navy Washington, D. C. 20007

13. ABSTRACT

The main results of a structural analysis program concerning a conventional submarine pressure hull configuration consisting of a rib-stiffened cylindrical shell with a reinforced circular penetration under hydrostatic pressure are discussed. The mathematical solution in series form has been obtained by superposing the analytical solutions for (a) a long, unstiffened, and unperforated circular cylindrical thin shell, closed at the ends, under external hydrostatic pressure, (b) a long, unstiffened, and unperforated circular cylindrical thin shell under a prescribed number of arbitrary radial line loads, and (c) a long, unstiffened, circular cylindrical shallow thin shell under arbitrary loading along the boundary of a circular penetration. During the computation, following truncation of the series, the method of least squares is employed in solving for the integration constants determined by the boundary conditions prescribed along the ribs and the reinforced penetration. The analysis has been coded and the numerical results generated by the use of a digital computer for an unstiffened as well as a rib-stiffened shell with a reinforced penetration are presented and compared graphically with experimental data available from certain photoelastic model tests. The corresponding zone of influence of the penetration and the state of stress concentration about it are delineated. (U)

DD FORM 1 JAN 64 1473

UNCLASSIFIED

Security Classification

14. KEY WORDS	LINK A		LINK B		LINK C	
	ROLE	WT	ROLE	WT	ROLE	WT
Submarine Pressure Hull Structure						
Reinforced Circular Opening						
Rib-Stiffened Cylindrical Shell						
Hydrostatic Pressure Loading						
Mathematical Stress Analysis						
Computer Solution Code						
Stress Concentration Factor						
Photoelastic Model Test						
Pressure Vessel Design						

INSTRUCTIONS

1. ORIGINATING ACTIVITY: Enter the name and address of the contractor, subcontractor, grantee, Department of Defense activity or other organization *(corporate author)* issuing the report.

2*a*. REPORT SECURITY CLASSIFICATION: Enter the overall security classification of the report. Indicate whether "Restricted Data" is included. Marking is to be in accordance with appropriate security regulations.

2*b*. GROUP: Automatic downgrading is specified in DoD Directive 5200.10 and Armed Forces Industrial Manual. Enter the group number. Also, when applicable, show that optional markings have been used for Group 3 and Group 4 as authorized.

3. REPORT TITLE: Enter the complete report title in all capital letters. Titles in all cases should be unclassified. If a meaningful title cannot be selected without classification, show title classification in all capitals in parenthesis immediately following the title.

4. DESCRIPTIVE NOTES: If appropriate, enter the type of report, e.g., interim, progress, summary, annual, or final. Give the inclusive dates when a specific reporting period is covered.

5. AUTHOR(S): Enter the name(s) of author(s) as shown on or in the report. Enter last name, first name, middle initial. If military, show rank and branch of service. The name of the principal author is an absolute minimum requirement.

6. REPORT DATE: Enter the date of the report as day, month, year, or month, year. If more than one date appears on the report, use date of publication.

7*a*. TOTAL NUMBER OF PAGES: The total page count should follow normal pagination procedures, i.e., enter the number of pages containing information.

7*b*. NUMBER OF REFERENCES: Enter the total number of references cited in the report.

8*a*. CONTRACT OR GRANT NUMBER: If appropriate, enter the applicable number of the contract or grant under which the report was written.

8*b*, 8*c*, & 8*d*. PROJECT NUMBER: Enter the appropriate military department identification, such as project number, subproject number, system numbers, task number, etc.

9*a*. ORIGINATOR'S REPORT NUMBER(S): Enter the official report number by which the document will be identified and controlled by the originating activity. This number must be unique to this report.

9*b*. OTHER REPORT NUMBER(S): If the report has been assigned any other report numbers *(either by the originator or by the sponsor)*, also enter this number(s).

10. AVAILABILITY/LIMITATION NOTICES: Enter any limitations on further dissemination of the report, other than those imposed by security classification, using standard statements such as:

(1) "Qualified requesters may obtain copies of this report from DDC."

(2) "Foreign announcement and dissemination of this report by DDC is not authorized."

(3) "U. S. Government agencies may obtain copies of this report directly from DDC. Other qualified DDC users shall request through
________________________."

(4) "U. S. military agencies may obtain copies of this report directly from DDC. Other qualified users shall request through
________________________."

(5) "All distribution of this report is controlled. Qualified DDC users shall request through
________________________."

If the report has been furnished to the Office of Technical Services, Department of Commerce, for sale to the public, indicate this fact and enter the price, if known.

11. SUPPLEMENTARY NOTES: Use for additional explanatory notes.

12. SPONSORING MILITARY ACTIVITY: Enter the name of the departmental project office or laboratory sponsoring *(paying for)* the research and development. Include address.

13. ABSTRACT: Enter an abstract giving a brief and factual summary of the document indicative of the report, even though it may also appear elsewhere in the body of the technical report. If additional space is required, a continuation sheet shall be attached.

It is highly desirable that the abstract of classified reports be unclassified. Each paragraph of the abstract shall end with an indication of the military security classification of the information in the paragraph, represented as *(TS), (S), (C), or (U)*.

There is no limitation on the length of the abstract. However, the suggested length is from 150 to 225 words.

14. KEY WORDS: Key words are technically meaningful terms or short phrases that characterize a report and may be used as index entries for cataloging the report. Key words must be selected so that no security classification is required. Identifiers, such as equipment model designation, trade name, military project code name, geographic location, may be used as key words but will be followed by an indication of technical context. The assignment of links, rules, and weights is optional.